



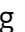





Vitamin D receptor enhances NLRC4 inflammasome activation by promoting NAIPs–NLRC4 association

Xin Chen^{1,†} , Zaikui Zhang^{1,†} , Naishuang Sun¹ , Jinzhou Li¹, Zemeng Ma¹ , Zebing Rao¹ , Xiaomeng Sun¹, Qiang Zeng¹, Yuxuan Wu¹, Jiahuang Li^{2,*} , Jing Zhang^{3,**}  & Yunzi Chen^{1,4,***} 

Abstract

Inflammasomes are cytosolic multiprotein complexes that initiate host defense against bacterial pathogens. The nucleotide-binding oligomerization domain (NOD)-like receptor (NLR) family caspase-associated recruitment domain-containing protein 4 (NLRC4) inflammasome plays a critical role in the inflammatory response against intracellular bacterial infection. The NLR family apoptosis inhibitory proteins (NAIPs) detect Flagellin or type III secretion system (T3SS) microbial components to activate NLRC4 inflammasome. However, the underlying mechanism of NLRC4 inflammasome activation is not completely understood. Here, we show that the vitamin D receptor (VDR) is an essential immunological regulator of the NLRC4 inflammasome. Conditional VDR knockout mice (VDR^{flox/flox} lyz2-Cre) exhibited impaired clearance of pathogens after acute *Salmonella Typhimurium* infection leading to poor survival. In macrophages, VDR deficiency reduced caspase-1 activation and IL-1 β secretion upon *S. Typhimurium* infection. For NAIPs act as upstream sensors for NLRC4 inflammasome assembly, the further study demonstrated that VDR promoted the NAIP–NLRC4 association and triggered NAIP–NLRC4 inflammasome activation, not NLRP3 activation. Moreover, Lys123 residue of VDR is identified as the critical amino acid for VDR–NLRC4 interaction, and the mutant VDR (K123A) effectively attenuates the NLRC4 inflammasome activation. Together, our findings suggest that VDR is a critical regulator of NAIPs–NLRC4 inflammasome activation, mediating innate immunity against bacterial infection.

Keywords NLRC4 inflammasome; *S. Typhimurium* infection; VDR

Subject Categories Immunology; Microbiology, Virology & Host Pathogen Interaction

DOI 10.15252/embr.202254611 | Received 4 January 2022 | Revised 19 June 2022 | Accepted 23 June 2022 | Published online 14 July 2022

EMBO Reports (2022) 23: e54611

Introduction

The NLR protein NLRC4 is a member of the NOD-like receptor family sensing a range of intracellular bacteria and plays a crucial role in the innate immune system. Ligands from Gram-negative bacteria such as needles and inner nod protein of the Type 3 secretion system (T3SS) can be detected by NAIPs. After detecting T3SS protein, NAIP associates with NLRC4 to induce the assembly of NAIP–NLRC4 inflammasome leading to caspase-1 activation. Activated caspase-1 processes IL-1 β release and triggers Gasdermin D (GSDMD)-mediated pyroptosis (Zhao *et al.*, 2011; Lage *et al.*, 2014; Vance, 2015; Zhao & Shao, 2015; Duncan & Canna, 2018; Bauer & Rauch, 2020; Gram *et al.*, 2021). Like all NLR family members, NLRC4 shares a typical three-domain structure: an N-terminal caspase-activation and recruitment domain (CARD), a central nucleotide-binding domain, and a C-terminal leucine-rich repeat (LRR) domain (Sundaram & Kanneganti, 2021). The activation of NLRC4 inflammasome requires NAIP proteins (NAIP1, NAIP2, NAIP5, and NAIP6 in mice) for sensing bacterial components in the cytosol (Gong & Shao, 2012; Lage *et al.*, 2014; Tenthorey *et al.*, 2014; Gram *et al.*, 2021). For bacteria that produce different amounts of multiple NAIP ligands with varying affinity, the degree of NLRC4 inflammasome activation is complex. Although the specific ligands for NLRC4 inflammasome have been examined in detail, the upstream regulators for NAIP–NLRC4 inflammasome assembly remain unclear and need further investigations.

More recent evidence demonstrates that vitamin D is an immunoregulatory hormone that modulates the innate and adaptive immune system (Gatti *et al.*, 2016; Carlberg, 2019; Ismailova & White, 2021). Vitamin D receptor (VDR) is a nuclear receptor and mediates the biological activity of vitamin D₃ (the active form of vitamin D). VDR deficiency is associated with inflammatory diseases, such as inflammatory bowel disease, sepsis, diabetes, and asthma (Liu *et al.*, 2013; Pappa, 2014; Madanchi *et al.*, 2018; Kim *et al.*, 2020). Vitamin D has been identified as a potent stimulator of

1 Key Laboratory of Immune Microenvironment and Disease, Department of Immunology, Nanjing Medical University, Nanjing, China

2 School of Biopharmacy, China Pharmaceutical University, Nanjing, China

3 The State Key Laboratory of Pharmaceutical Biotechnology, School of Life Sciences, Nanjing University, Nanjing, China

4 Medical Centre for Digestive Diseases, Second Affiliated Hospital of Nanjing Medical University, Nanjing, China

*Corresponding author. Tel: +86 25 86185986; E-mail: lijiah@cpu.edu.cn

**Corresponding author. Tel: +86 25 89683692; E-mail: jzhang08@njmu.edu.cn

***Corresponding author. Tel: +86 25 86869454; E-mail: chenyunzi@njmu.edu.cn

†These authors contributed equally to this work

[Correction added on July 21st 2022, after first online publication: deleted “the” in Heading]

autophagy in infection and HIV infection (Ismailova & White, 2021). VDR negatively regulated bacteria-induced NF- κ B activity in intestinal inflammation (Wu *et al.*, 2010). We previously reported that VDR inhibits NLRP3 inflammasome activation (Rao *et al.*, 2019). We investigated whether VDR has a similar role in NLRC4 inflammasome activation for its importance in cellular immunity.

Here, we report a novel role of VDR in the optimal activation of the NLRC4 inflammasome. Our findings show that VDR promotes ligand-bound NAIP association with NLRC4 and enhances the activation of NLRC4 inflammasome, contributing to host defense against bacterial pathogens.

Results

VDR deficiency impairs NLRC4-dependent inflammasome activation

To determine the role of VDR in NLRC4 inflammasome activation, we first examined inflammasome activation in response to

Salmonella Typhimurium infection in VDR-deficient and WT BMDMs. VDR-deficient macrophages showed reduced pro-caspase-1 activation and Gasdermin D cleavage (Fig 1A), IL-1 β and IL-18 secretion (Fig 1B and C), and LDH release (Fig 1E), but no changes in TNF α production compared with WT macrophages (Fig 1D), indicating the defective effect specific to inflammasome activation. Consistently, the recovery expression of VDR in *Vdr*^{-/-} BMDMs rescued the caspase-1 activation and IL-1 β production (Fig 1F). Using NLRC4 inflammasome-specific ligands (Flic and PrgJ) to induce NLRC4 inflammasome activation, similar results were observed in *Vdr*^{-/-} BMDMs (Fig 1G). To further examine whether VDR is involved in NLRC4 inflammasome activation, BMDMs from *Nlr4*^{-/-} and *Nlr4*^{-/-} *Vdr*^{-/-} mice were prepared for FLIC stress, *Nlr4*^{-/-} and *Nlr4*^{-/-} *Vdr*^{-/-} BMDMs showed similar inflammasome activation defects in response to FLIC (Fig 1H-L). In addition, we tested the role of VDR in NLRC4 inflammasome activation in human cells and examined the caspase-1 and IL-1 β cleavage in response to *S. Typhimurium* infection in VDR-deficient (sh-VDR) and control THP-1 cells; VDR-deficient THP-1 cells showed reduced pro-caspase-1 and pro-IL-1 β

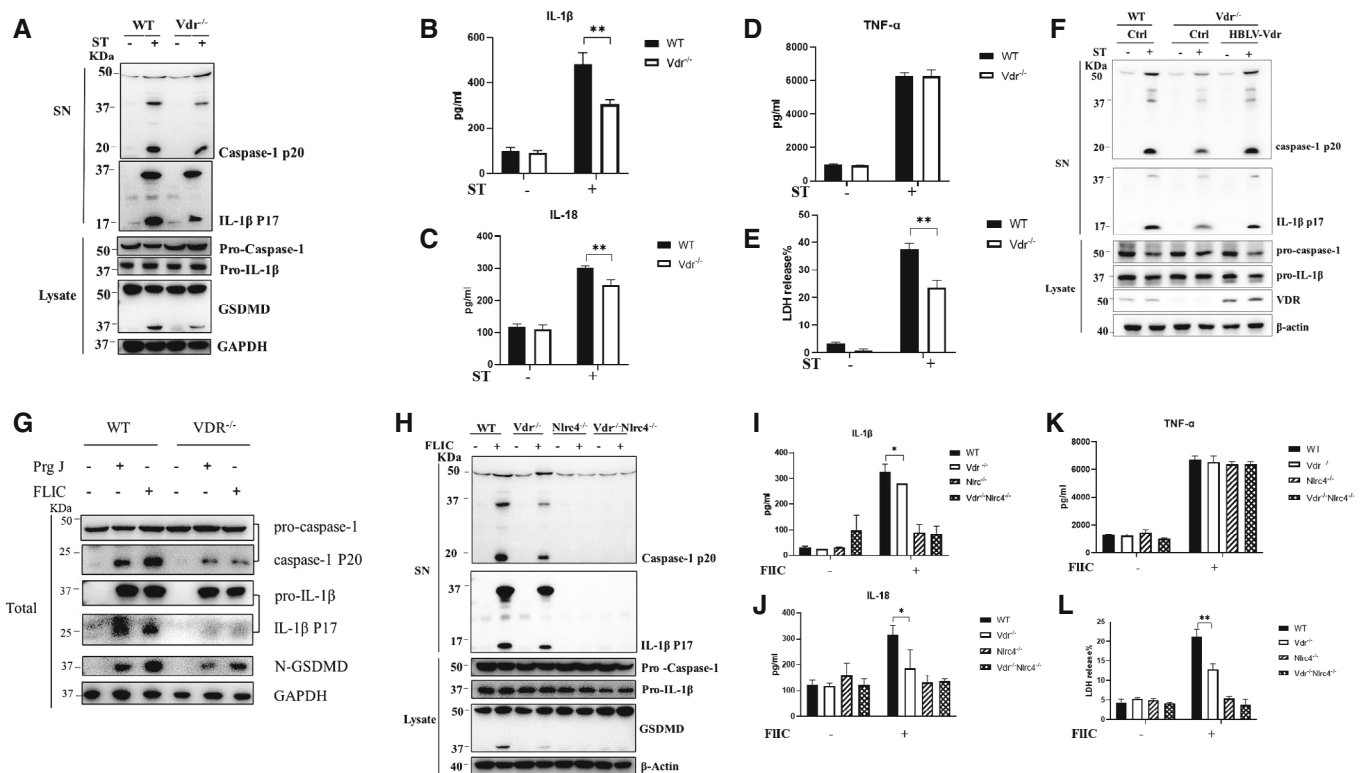


Figure 1. VDR deficiency impairs NLRC4-dependent inflammasome activation.

A–H LPS-primed WT and *Vdr*^{-/-} BMDMs were infected with 50 MOI *S. Typhimurium* for 2 h. Culture supernatants (SN) and cell lysates (Lysate) were collected and immunoblotted with the indicated antibodies (A). (B–E) IL-1 β secretion (B), IL-18 secretion (C) and TNF- α secretion (D) and LDH release (E) in supernatants. (F) HBLV-Vdr expression in *Vdr*^{-/-} BMDMs by lentivirus-mediated transduction primed with LPS and infected with 50 MOI *S. Typhimurium* for 2 h, cell lysates, and culture supernatants (SN) were collected and immunoblotted with the indicated antibodies. (G) LPS-primed WT and *Vdr*^{-/-} BMDMs were treated with 1 μ g/ml FLIC (LFn-Flagellin and PA) or PrgJ (1 μ g/ml LFn-PrgJ and PA) for 1 h, total mixtures (culture supernatants and cell lysates) were collected and immunoblotted with the indicated antibodies. (H) LPS-primed WT, *Vdr*^{-/-}, *Nlr4*^{-/-} and *Vdr*^{-/-} *Nlr4*^{-/-} BMDMs were treated with FLIC for 1 h, Culture supernatants (SN) and cell lysates were collected and immunoblotted with the indicated antibodies. I–L IL-1 β secretion (I), IL-18 secretion (J) and TNF- α secretion (K) and LDH release (L) in supernatants. Data are shown as means \pm SEM; determined by Student's *t*-test; *, $P < 0.05$; **, $P < 0.01$. In each panel, data are representative of at least three independent experiments.

Source data are available online for this figure.

activation (Fig EV1A), and LDH release (Fig EV1B). Collectively, these data indicate that VDR is required for the optimal activation of the NLRC4 inflammasome.

VDR is involved in host defense against *S. Typhimurium* infection, independent of NLRP3

Then, we sought to determine whether VDR deficiency in macrophages reduces NLRC4 inflammasome activation *in vivo*. Conditional knockout VDR transgenic mice (VDR^{flox/flox} lyz2-Cre) were generated via crossing VDR-floxed mice with lyz2-Cre mice (Fig EV2A and B). The peritonitis was induced in VDR^{flox/flox} lyz2-Cre and the littermate control mice (VDR^{flox/flox}) by intraperitoneal injection with 10⁷ CFUs of *S. Typhimurium*. After 6-h infection, IL-1 β levels were significantly reduced in the peritoneal cavity-flushed fluids (PCFs) and the sera from VDR^{flox/flox} lyz2-Cre mice compared with control mice (Fig 2A and C). Meanwhile, TNF α levels showed no differences between the two groups of mice, supporting that the effect of VDR is specific to inflammasome activation (Fig 2B and D). The previous study showed that IL-1 β is essential for controlling the infection, and NLRC4-

dependent IL-1 β production from the neutrophils is crucial for protecting mice in the *S. Typhimurium*-induced peritonitis model (Liu *et al*, 2017), so we examined the recruitment of peritoneal neutrophils. The sorted neutrophils (CD11b⁺Ly6G⁺ cells) VDR^{flox/flox} lyz2-Cre mice were reduced compared with control mice (Fig 2E). The bacterial colonization was increased in the blood, PCF, and spleen from VDR^{flox/flox} lyz2-Cre mice bearing *S. Typhimurium*-induced peritonitis model (Fig 2F and G). Moreover, 60% of VDR^{flox/flox} lyz2-Cre mice died after 4 days of infection, while 80% of control mice remained alive (Fig 2H). These data indicate that VDR protection against *S. Typhimurium* infection in mice may be associated with the NLRC4-inflammasome activation.

The previous report showed that NLRP3 partially participates in NLRC4-dependent inflammasome activation (Qu *et al*, 2016). To address whether NLRP3 is involved in VDR-mediated inflammasome activation, BMDMs from VDR^{-/-}Nlrp3^{-/-}, Nlrp3^{-/-}, VDR^{-/-}, and WT mice were prepared for *S. Typhimurium* infection. The results showed similar responses between Nlrp3^{-/-} and WT BMDMs, and VDR^{-/-} and VDR^{-/-}Nlrp3^{-/-} BMDMs also showed similar responses to *S. Typhimurium* infection, such as caspase-1

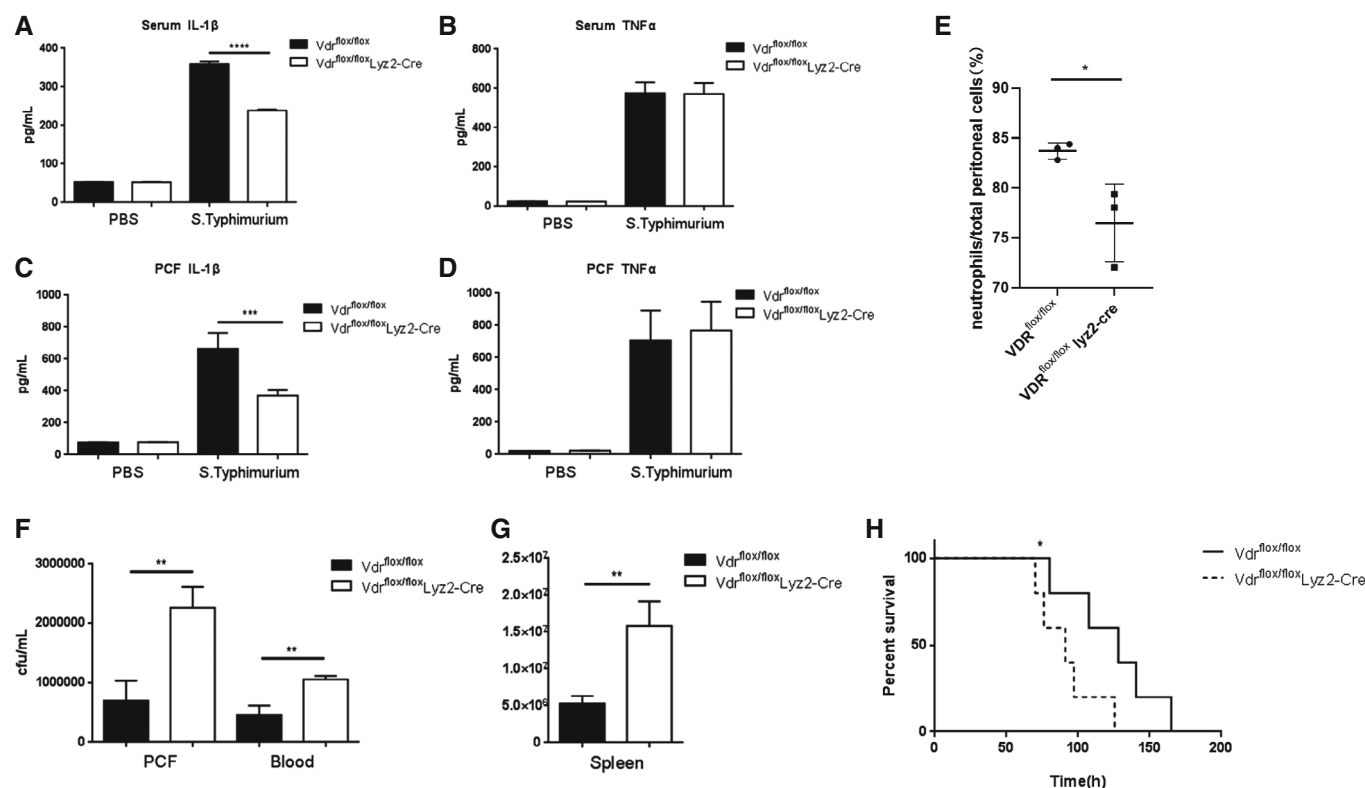


Figure 2. VDR is involved in host defense against *S. Typhimurium* infection.

A–H IL-1 β (A) and TNF- α (B) levels in sera and IL-1 β (C) and TNF- α (D) in PCF of littermate VDR^{flox/flox} and VDR^{flox/flox} lyz2-Cre mice 6 h after *S. Typhimurium* (10⁷ CFUs/mouse) infection with ELISA detecting. (E) The absolute number of neutrophils (CD11b⁺Ly6G⁺) from PCF of VDR^{flox/flox} and VDR^{flox/flox} lyz2-Cre mice 6 h after *S. Typhimurium* infection. (F) Bacterial burden in blood, PCF, and spleen (G) of VDR^{flox/flox} and VDR^{flox/flox} lyz2-Cre mice 24 h after *S. Typhimurium* infection. (H) Survival of littermate VDR^{flox/flox} and VDR^{flox/flox} lyz2-Cre mice infected intraperitoneally with *S. Typhimurium* (10² CFUs/mouse). Data in (A–H) are shown as means \pm SEM; determined by Student's *t*-test; **P* < 0.05; ***P* < 0.01; ****P* < 0.001; *****P* < 0.0001 or the Kaplan–Meier method (H). Data in (A–F) are representative of at least three independent experiments, and *n* = 5 mice/group (A–D, F–G) or *n* = 3 mice/group (E); data in (H) are representative of two independent experiments, and *n* = 10 mice/group.

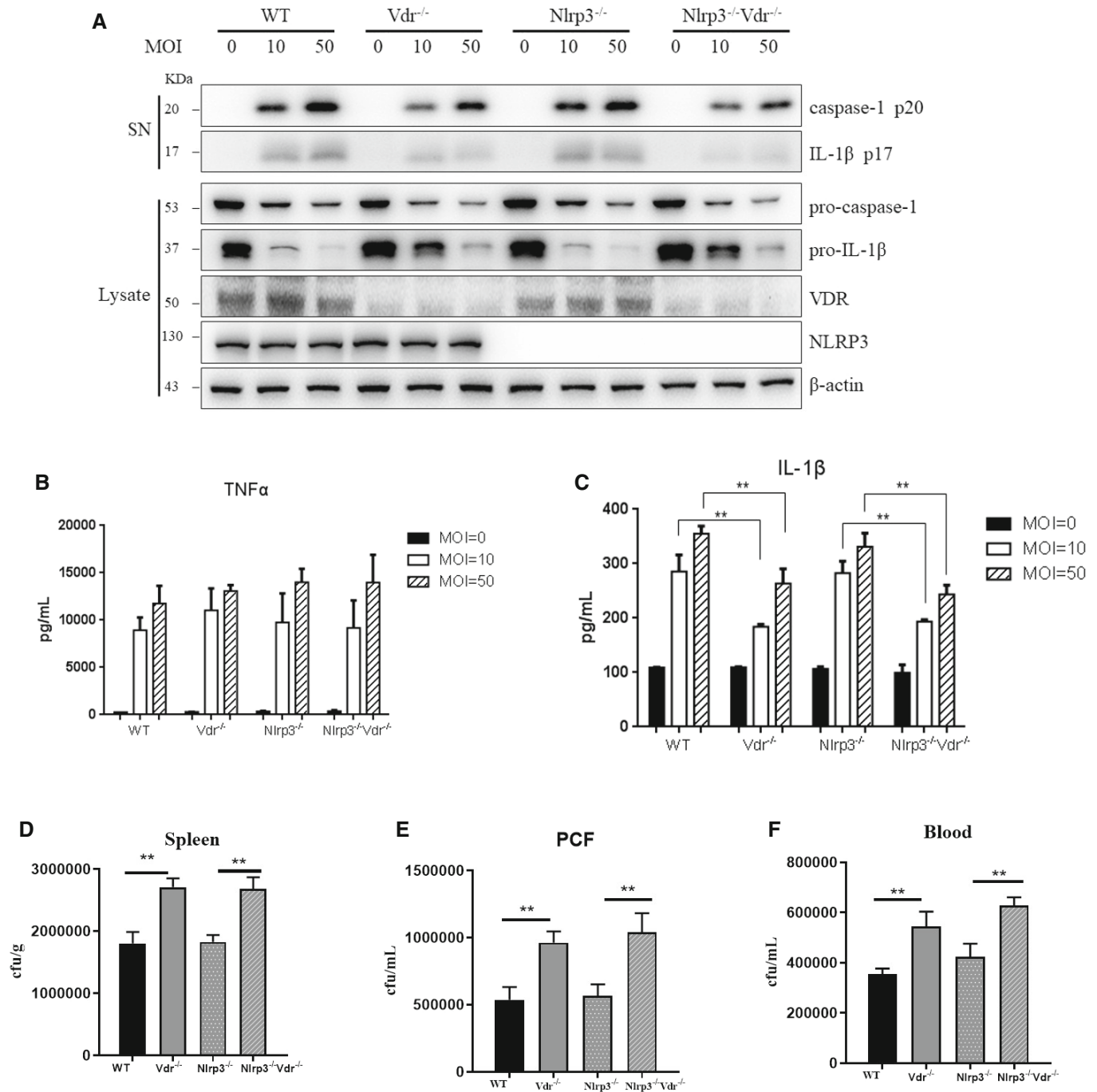


Figure 3. NLRP3 is not involved in the protective role of VDR in the defense against *S. Typhimurium* infection.

A–F LPS-primed WT, Vdr^{-/-}, NLRP3^{-/-} and NLRP3^{-/-} Vdr^{-/-} BMDMs were infected with different MOI (0, 10, 50) *S. Typhimurium* for 2 h. Culture supernatants (SN) and Cell lysates were collected and immunoblotted with the indicated antibodies (A). ELISA detected TNF- α (B) and IL-1 β (C) in supernatants. Bacterial burden was detected in spleens (D), PCF (E), and blood (F) of WT, Vdr^{-/-}, NLRP3^{-/-}, and NLRP3^{-/-} Vdr^{-/-} mice 24 h after *S. Typhimurium* infection.

Data information: $n \geq 3$ biological replicates. Data are presented as the mean \pm SEM; determined by Student's *t*-test; ** $P < 0.01$.

Source data are available online for this figure.

cleavage, TNF α and IL-1 β secretion (Fig 3A–C). Then, *in vivo* assays by intraperitoneal injection of *S. Typhimurium* into mice, the bacterial colonization in blood, PCF, and spleen displayed no significant

differences between VDR^{-/-}Nlrp3^{-/-} and VDR^{-/-} mice (Fig 3D–F). These data suggest that NLRP3 is not involved in the protective role of VDR in the defense against *S. Typhimurium* infection.

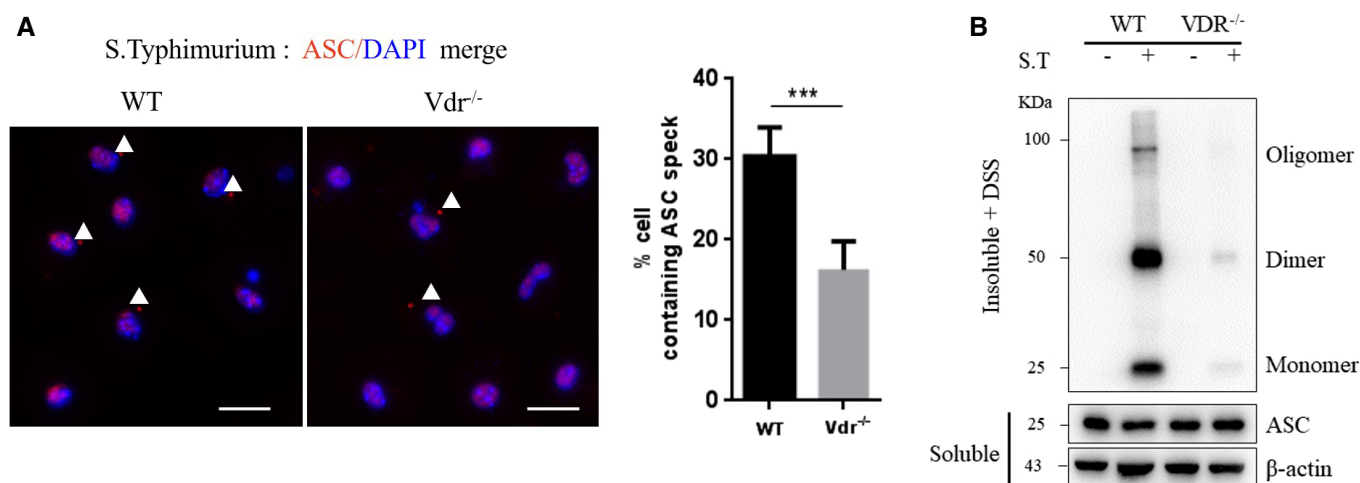


Figure 4. VDR deficiency reduces ASC speck formation upon NLRC4 inflammasome activation.

A LPS-primed WT and *Vdr*^{-/-} BMDMs were infected with *S. Typhimurium* at an MOI of 50 for 2 h. Endogenous ASC specks (arrows) were represented and quantified by immunofluorescence images. The data show representative results from three independent experiments: scale bar, 20 μ m. Data are presented as the mean \pm SEM; determined by Student's *t*-test, ***, *P* < 0.001.

B ASC oligomerization induced by the indicated stimuli in WT and *Vdr*^{-/-} BMDMs primed with LPS.

VDR deficiency reduces ASC speck formation upon NLRC4 inflammasome activation

The activation of NLRC4 leads to the assembly of a macromolecule complex containing ASC formation (the adapter for inflammasome complex; Broz *et al*, 2010). Activated NLRC4 can associate with ASC and colocalizes with the ASC-containing speck during *S. Typhimurium* infection (Vance, 2015). The effect of VDR on the ASC formation during NLRC4 inflammasome activation was examined in VDR-deficient and WT macrophages. Upon *S. Typhimurium* infection, endogenous ASC specks were visualized by immunofluorescence staining. Compared with WT macrophages, the frequency of ASC speck-containing cells was significantly decreased in VDR-deficient macrophages (Fig 4A), suggesting that VDR is required for ASC speck formation upon NLRC4 inflammasome activation.

For the ASC specks are oligomers of ASC protein that manifest as Triton X-100-insoluble aggregates, we analyzed the Triton X-100-soluble and TritonX-100-insoluble fractions from macrophages by Western blot. Consistent with fluorescent observation, the reduced oligomerization of ASC was detected in VDR-deficient macrophages infected with *S. Typhimurium*, and its oligomer (Fig 4B). These data suggest that VDR participates in the assembly of the ASC–NLRC4 complex.

VDR interacts with NLRC4

To illustrate the mechanism of VDR enhancing NLRC4 inflammasome activation, we checked the expression of genes related to the NLRC4 inflammasome in the absence of VDR. The results showed no significant difference in the expression of these genes, including NLRC4, pro-caspase-1, pro-IL-1 β , Gasdermin D, ASC, NAIP2, and NAIP5 in WT and *Vdr*^{-/-} BMDMs (Fig EV3A–D). Based on the above result of the reduced ASC speck formation in VDR-deficient macrophages, further examination was focused on the

interaction between the VDR and NLRC4 inflammasome. Co-immunoprecipitation (Co-IP) experiments indicated that endogenous VDR interacted with NLRC4 in BMDMs (Fig 5A) and THP-1 cells (Fig EV1C and D). The VDR–NLRC4 association was confirmed by co-IP assays in HEK293T cells with Flag-VDR and Myc-NLRC4 overexpression (Fig 5B and C) and visualized by immunofluorescence assays (Fig EV2C). In addition, *in vitro* assay with recombinant GST-VDR protein further demonstrated that VDR interacted directly with NLRC4 (Fig 5D). To map the domain of NLRC4 required for the interaction with VDR, we generated a series of NLRC4 truncations, and the Co-IP assay showed that the NACTH and LRR domain of NLRC4 interacted with VDR (Fig 5E). For VDR, the LBD domain of VDR (LBD-VDR) was detected in the NLRC4 immunoprecipitation (Fig 5F). In addition, we also found that VDR had no effect on the phosphorylation of NLRC4 at Ser533 (Fig EV4), which is critical for the NLRC4 inflammasome activation following infection with *S. Typhimurium* (22, 23). Considering the LRR or NACTH domain of NLRC4 sequesters the protein as a monomeric state in an auto-inhibitory conformation (Zhang *et al*, 2015), we speculate that the self-inhibition of NLRC4 can be relieved by VDR interaction with the LRR or NACTH domain of NLRC4, contributing to the NLRC4 inflammasome activation.

VDR enhances NAIPs–NLRC4 complex formation

NAIPs function as receptors for microbial molecules in the inflammasome pathway. The specific ligand-receptor ligation stimulates a physical association of the NAIP with NLRC4 and undergoes oligomerization to form the inflammasome complex for caspase-1 activation. NAIP5 and its paralog in mice (NAIP2) recognize flagellin and the T3SS rod protein (Bauer & Rauch, 2020). We further investigate whether VDR is required to form the NAIP5/NAIP2 and NLRC4 complex. In co-IP assays, besides Flagellin and PrgJ in the immunoprecipitated complex of NLRC4, we found that VDR

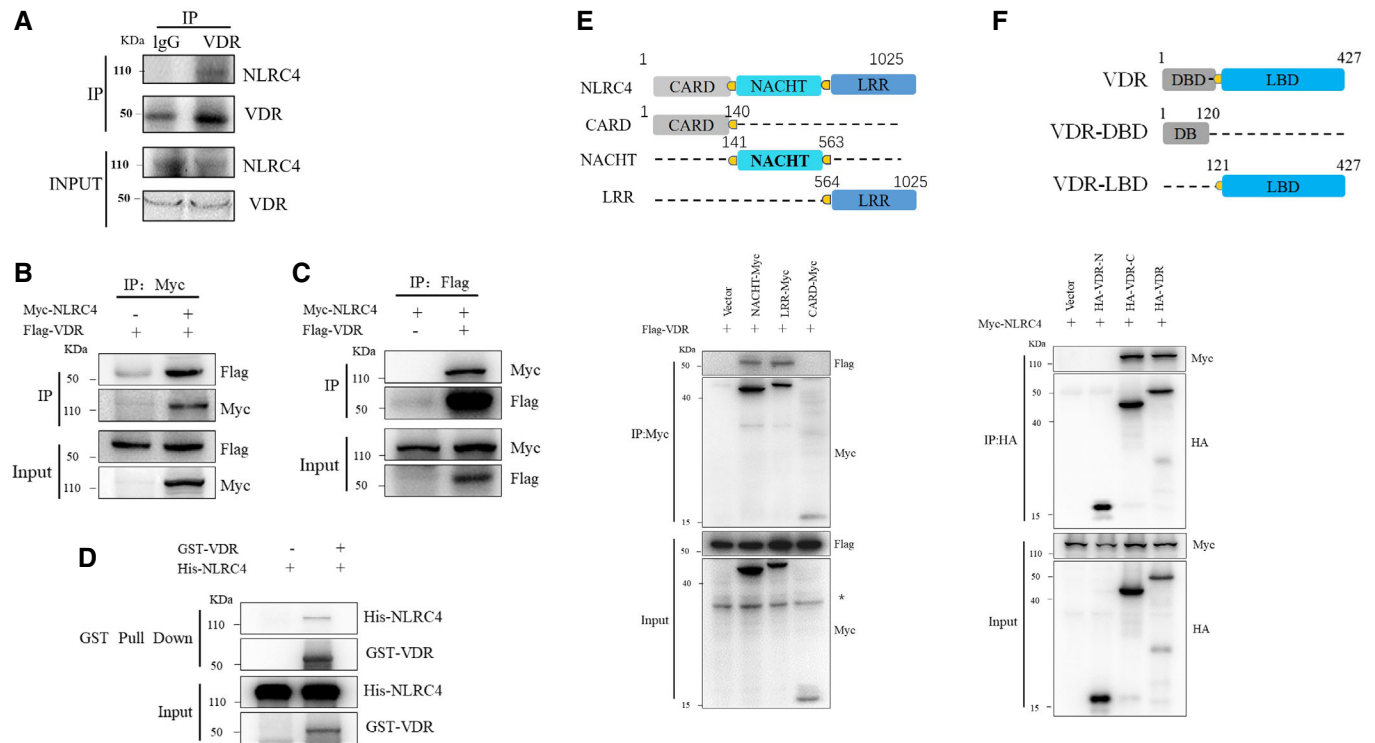


Figure 5. VDR interacts with NLRC4.

A–F LPS-primed BMDMs were infected with *S. Typhimurium* at an MOI of 50 for 2 h. Lysates were immunoprecipitated (IP) using an anti-VDR antibody and were immunoblotted with the indicated antibodies (A). Whole-cell lysates were shown as the input. (B, C) Flag-VDR was co-expressed with Myc-NLRC4 in HEK293T cells; proteins were immunoprecipitated and analyzed by immunoblotting with indicated antibodies. Whole-cell lysates were shown as the input. (D) Purified GST-VDR was incubated with purified His-NLRC4 for 2 h. His-NLRC4-bound to GST-VDR was pulled down by glutathione beads and subjected to immunoblot analysis. (E) WT or mutant NLRC4 (CARD, NACHT, or LRR (leucine-rich repeat)) and HA-VDR were expressed in HEK293T cells, immunoprecipitated, and analyzed by immunoblotting with indicated antibodies. *no specific band. (F) WT or mutant VDR (DBD or LBD) and Myc-NLRC4 were expressed in HEK293T cells, immunoprecipitated, and analyzed by immunoblotting with indicated antibodies. Data are representative of three independent experiments.

overexpression increased the interaction between NAIP5/NAIP2 and NLRC4 upon flagellin or PrgJ stimulation (Fig 6A and B). As mentioned above, LBD-VDR is necessary for VDR to associate with NLRC4, so a similar result was confirmed by LBD-VDR overexpression. LBD-VDR also enhanced the formation of the NAIP5/NAIP2–NLRC4 complex (Fig 6C and D). These results indicate that the role of VDR in the NLRC4 inflammasome pathway is to improve the NAIP5/NAIP2–NLRC4 complex formation.

Lys123 of VDR is the critical amino acid required for the regulation of NLRC4 inflammasome activation

To clarify the molecular mechanism of VDR in the regulation of NLRC4 inflammasome activation, we used molecular docking to predict the critical binding site of VDR in the NLRC4 inflammasome formation. According to the calculation results, Lys123 residue of VDR has a high frequency as a protein–protein interaction site for NLRC4 (Fig EV5A–C). Predicted results indicated that Lys123 of VDR binds to Glu327 in the HD1 region of NLRC4 via an ionic bond, Gln324 and Asp597 in the LRR region via hydrogen bonds to stabilize the active conformation of NLRC4 (Fig 7A). Then, we constructed VDR (K123A) mutant to study VDR–NLRC4 interaction to testify to this prediction. As expected,

VDR (K123A) showed a weak interaction with NLRC4 (Fig 7B). For PrgJ–NAIP2–NLRC4 complex formation, the inflammasome assembly was enhanced by VDR, not by VDR (K123A; Fig 7C), and when VDR (K123A) transfection into VDR^{−/−} iBMDMs in response to *S. Typhimurium* infection, the activation of Caspase-1, IL-1 β and IL-18 production, Gasdermin D cleavage, and LDH release were decreased compared with VDR^{−/−} iBMDMs (Fig 7D–G), but no changes in TNF α production (Fig 7H). In conclusion, Lys123 is the critical amino acid of VDR for NLRC4 inflammasome activation.

Discussion

There is an emerging role for vitamin D3 in the innate immune system wherein it may influence cellular sensing and responses of macrophages and dendritic cells (13). Vitamin D receptors (VDR) are also identified in various immune cells and possess immunomodulatory properties. VDR deficiency is associated with increased inflammation and deregulation in inflammatory diseases, such as inflammatory bowel disease, sepsis, diabetes, and asthma (21). We established a VDR^{flox/flox} Lyz2-Cre mouse model with selective KO of VDR expression in macrophages to investigate the role of

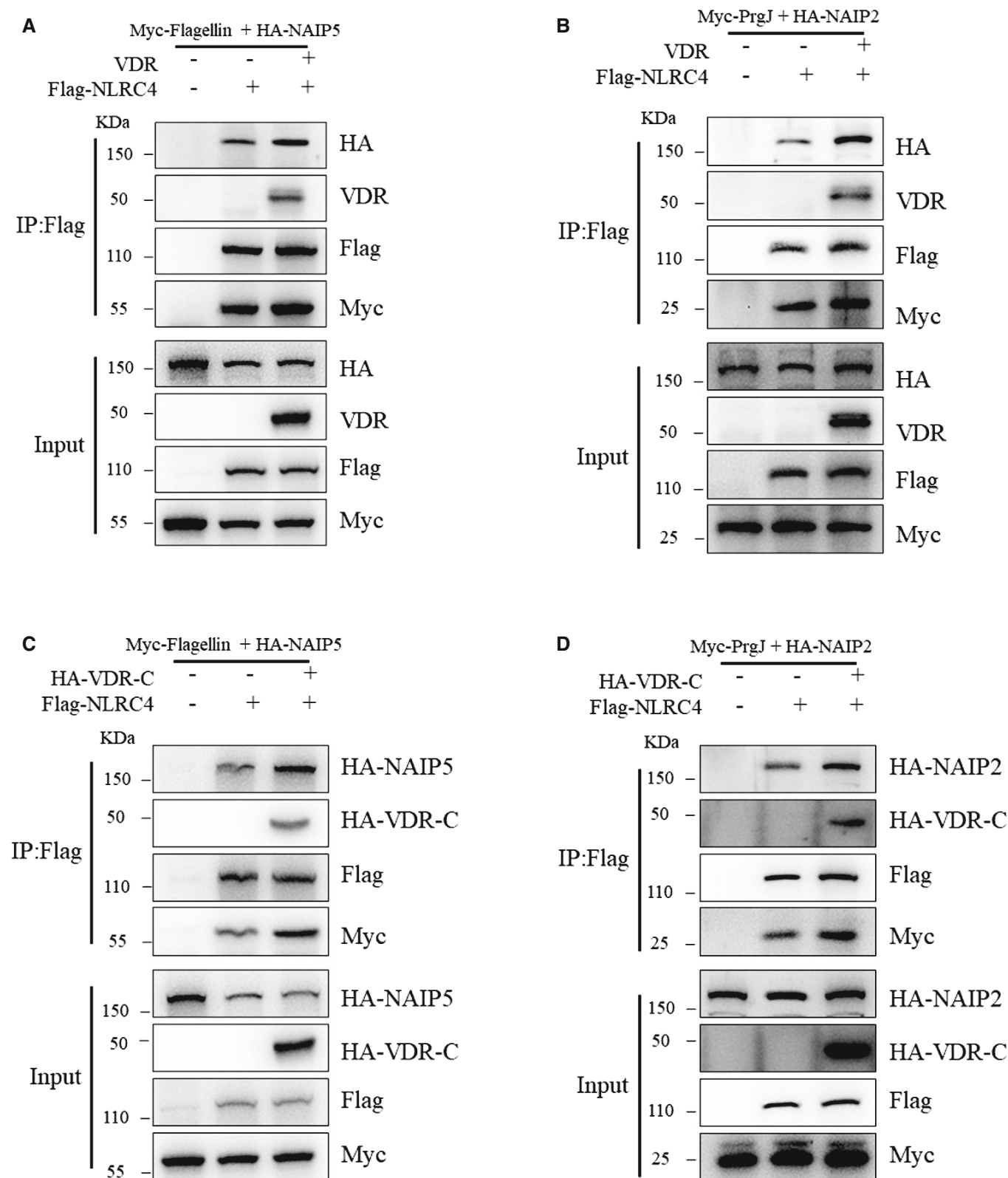


Figure 6. VDR enhances NAIP interaction with NLRC4.

A–D HEK293T cells were transfected with Flag-NLRC4, VDR, Myc-Flagellin, and HA-NAIP5 (A) or Flag-NLRC4, VDR, Myc-PrgJ and HA-NAIP2 (B), or Flag-NLRC4, LBD-VDR, Myc-Flagellin, and HA-NAIP5 (C) or Flag-NLRC4, LBD-VDR, Myc-PrgJ, and HA-NAIP2 (D). Samples were immunoprecipitated with the anti-Flag and analyzed by immunoblotting with indicated antibodies.

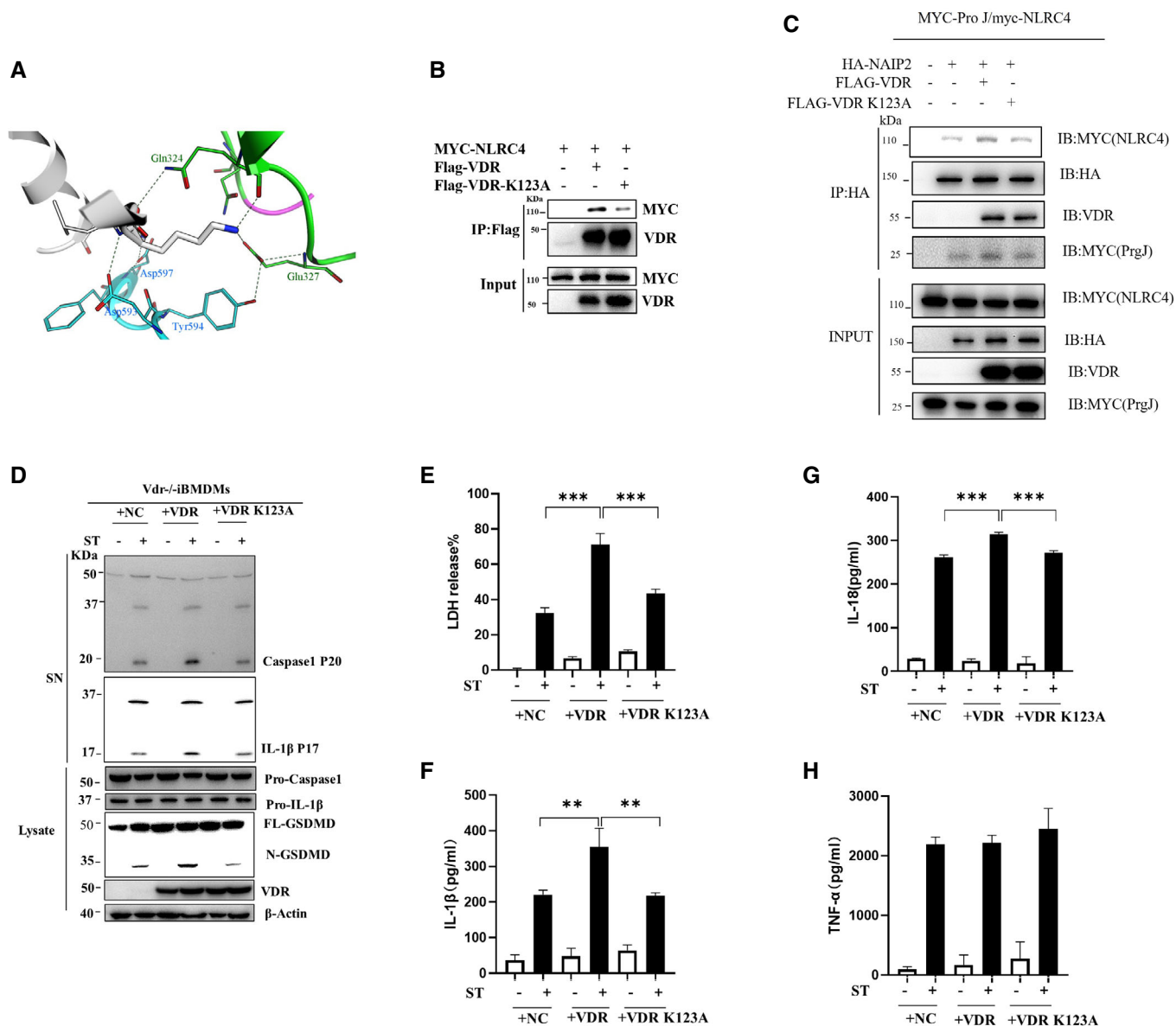


Figure 7. VDR K123A mutation attenuates VDR regulation of NLRC4 inflammasome activation.

- A Predict possibility of interaction amino acids between lys123 of VDR and NLRC4.
 B VDR or mutant VDR (K123A) and Myc-NLRC4 were expressed in HEK293T cells, immunoprecipitated with the anti-Flag antibody, and analyzed by immunoblotting with indicated antibodies.
 C Transfected VDR or mutant VDR (K123A) and Flag-NLRC4, Myc-PrgJ, and HA-NAIP2 in HEK293T cells, immunoprecipitated with the anti-HA antibody, and analyzed by immunoblotting with indicated antibodies.
 D Vdr^{-/-} BMDMs were infected with lentivirus, which expressed Vector (NC), VDR, and VDR-K123A, infected with *S. Typhimurium* at an MOI of 50 for 2 h, cell lysates (Lysate) and culture supernatants (SN) were collected and immunoblotted with the indicated antibodies.
 E–H LDH release (E), IL-1 β secretion (F), IL-18 secretion (G) and TNF- α secretion (H) in supernatants. Data are shown as means \pm SEM; determined by Student's *t*-test; **, $P < 0.01$; ***, $P < 0.001$; In each panel, data are representative of at least three independent experiments.

Source data are available online for this figure.

VDR on the innate immune against *S. Typhimurium* infection. Our findings demonstrate that VDR acts as an endogenous regulator of NAIP–NLRC4 inflammasome assembly to modulate NLRC4 activation in the host defense against *S. Typhimurium* infection.

NLRC4 inflammasomes are activated by bacterial pathogens carrying Flagellin or the type III secretion system (T3SS) (22, 23).

The specificity of the NLRC4 inflammasomes is dictated by the NAIPs sensor for different bacterial ligands (3, 4, 7). NAIP proteins possess a catalytic surface matching the oligomerization surface of NLRC4 to initiate NLRC4 oligomerization (24). Our results showed that VDR enhanced NAIPs binding to the NLRC4 complex via interaction with NLRC4 and promoted the NLRC4 oligomerization.

During the activation of NLRC4, inactive NLRC4 is catalyzed to its active conformation and then self-propagates the active conformation to form the wheel-like architecture. We speculate that VDR binding to the LRR or NACTH domain of NLRC4 might help change the auto-inhibitory conformation of NLRC4 (Fig 5). Based on the computing analysis of the spatial structure of the NLRC4–VDR association, the prediction indicates Lys123 as the critical amino acid for the formation of the VDR–NLRC4 complex. As Lys residue commonly acts as a ubiquitination site for posttranslational processing, Western blot analysis indicated no difference in the ubiquitination of the two proteins, VDR and VDR (K123A; Fig EV5D). However, the importance of Lys123 for VDR in the regulation of NLRC4 inflammasome activation was demonstrated by *in vitro* and *in vivo* assays (Fig 7).

Our previous study reported VDR as a negative NLRP3 oligomerization and activation; in the absence of VDR, NLRP3 inflammasome activation was increased in response to LPS-induced or alum-induced peritoneal inflammation (Rao et al, 2019). Similar studies have reported that the VDR agonist exerts an inhibitory effect on NLRP3 inflammasome activation, and vitamin D3 can abolish NLRP3 inflammasome activation and inhibit caspase-1 activation

and IL-1 β secretion via VDR function (Duan et al, 2021). However, in the *S. Typhimurium*-induced peritonitis model, our results showed that the IL-1 β production and caspase-1 cleavage were no significant differences between VDR^{-/-} and NLRP3^{-/-} VDR^{-/-} macrophages, even between NLRP3^{-/-} and WT macrophages, demonstrating macrophages response to *S. Typhimurium* infection is not NLRP3-dependent process. In addition, the phosphorylation of NLRC4 at S533 was reported to recruit ASC to activate inflammasome by interacting with NLRP3 (Qu et al, 2016). Here, we found that VDR does not affect NLRC4 phosphorylation, further confirming that the regulation of VDR on NLRC4 inflammasome activation is independent of the NLRP3 signal.

Collectively, our findings provide a novel role of VDR in NLRC4 inflammasome activation in response to intracellular bacterial infection. Of note, VDR exerts the opposite effect in two inflammasomes, inhibiting NLRP3 activation but promoting NLRC4 activation. VDR is a vital regulator for host cells responding to pathogenic insults. Insights gained from understanding how the VDR pathway is integrally involved in regulating inflammasome activation may deepen the understanding of the nature of host defense signals in inflammation.

Materials and Methods

Reagents and Tools table

Reagent or resource	Source	Identifier
Antibodies		
Anti-NLRC4 (human)	Cell signaling technology	Cat#3724
Anti-NLRC4 (human & mouse)	EMD Millipore	Cat#2994846
Anti-GSDMD	Abcam	Cat#ab209845
Anti-p-NLRC4 (Ser533)	ECM Biosciences	Cat#5411
Anti-HA	Cell signaling technology	Cat#3724
Anti-Myc	Thermo Fisher	Cat# MA1-980
Anti-Myc	Proteintech	Cat# 10828-1-AP
Anti-Flag	Sigma	Cat# F1804
Anti-NLRP3/NALP3	AdipoGen	Cat# AG-20B-0014
Anti-VDR	Santa Cruz	Cat# sc-13133
Anti-VDR	Proteintech	Cat#14526-1-AP
Anti- β -actin	Santa Cruz	Cat# sc-47778
Anti-Caspase-1 (mouse)	AdipoGen	Cat# AG-20B-0044
Anti-ASC	AdipoGen	Cat# sc-514414
Anti-IL-1 β	R&D Systems	Cat# AF-401-NA
Bacterial and virus strains		
<i>Salmonella Typhimurium</i> SL1344	ATCC	14028

Reagents and Tools table (continued)

Reagent or resource	Source	Identifier
Experimental models: cell lines		
HEK HEK293T cell	ATCC	CRL-11268
THP1 cell	ATCC	TIB-202
Critical commercial assays		
TNF ELISA kit	BD Biosciences	Cat#558534
Mouse IL-1 β ELISA kit	BD Biosciences	Cat#559603
TMB substrate reagent set	BD Biosciences	Cat#555214
Mouse IL-18 ELISA kit	MBio	Cat#CK-E 20173
LDH cytotoxicity detection kit	Beyotime	Cat#C0017
Experimental models: organisms/strains		
Mouse: Nlrp3 ^{-/-}	Dr. Shuo Yang	N/A
Mouse: Vdr ^{-/-}	The Jackson Laboratory	JAX:017969
Mouse: Lys2-Cre	The Jackson Laboratory	Stock No:004781
Nlrc4 ^{-/-}	Dr. Feng Shao	N/A
Vdr ^{flox/flox}	Beijing Biocytogen	N/A
Recombinant DNA		
HA-ASC	Professor Paul N. Moynagh (National University of Ireland Maynooth, Ireland)	N/A
pCMV-HA-VDR	This paper	N/A
pCMV-HA-VDR-C terminal	This paper	N/A
pCMV-HA-VDR-N terminal	This paper	N/A
pcNDA3.1-Flag-VDR	This paper	N/A
pcNDA3.1-Flag-VDR-C terminal	This paper	N/A
pcNDA3.1-Flag-VDR-N terminal	This paper	N/A
Pgex6p1-GST-VDR	This paper	N/A
pcDNA3.3-Myc-NLRC4	This paper	N/A
pcDNA3.3-Myc-CARD	This paper	N/A
pcDNA3.3-Myc-NACHT	This paper	N/A
pcDNA3.3-Myc-LRR	This paper	N/A
Pet28a-His-NLRC4	This paper	N/A
Myc-PrgJ	Dr. Feng Shao (NIBS)	N/A
Myc-Flagellin	Dr. Feng Shao (NIBS)	N/A
HA-NAIP2	Dr. Feng Shao (NIBS)	N/A
HA-NAIP5	Dr. Feng Shao (NIBS)	N/A
PET28-Lfn- Flagellin	Dr. Feng Shao (NIBS)	N/A
PET28-Lfn-PrgJ	Dr. Feng Shao (NIBS)	N/A
PET28- anthrax-protective antigen	Dr. Feng Shao (NIBS)	N/A
Flag-NLRC4	Dr. Feng Shao (NIBS)	N/A
Oligonucleotides		
Primer for mouse Naip2: Forward: CCAAATCATCTGTGCCCAA; Reverse: ATGCCCTGACCTGTTTGT	This paper	N/A
Primer for mouse Naip5: Forward: CTGCTCACCTTCCCTTTA; Reverse: GGTCTTAGTCGTTGGCTTC	This paper	N/A

Reagents and Tools table (continued)

Reagent or resource	Source	Identifier
Primer for mouse Nlrc4: Forward: TATGACCGAAGACAGTCCCA; Reverse: TGTATCAGGAGTCGTAGAAGG	This paper	N/A
Primer for ShRNA-hVdr: Forward: GATCCCTCCAGTTCGTGTGAATGATCTCGAGATCATTACACGAACTGGAGGTTTTTC Reverse: TCGAGAAAAACCTCCAGTTCGTGTGAATGATCTCGAGATCATTACACGAACTGGAGGG	This paper	N/A

Methods and Protocols

Study design

This study evaluated the protective effect of VDR on *Salmonella* infection and explored the mechanism by which VDR affects NLRC4 inflammasome activation. The effect of VDR on activation of the NLRC4 inflammasome in mouse BMDMs and the underlying mechanism of action were studied using immunoblotting, enzyme-linked immunosorbent assay (ELISA), co-immunoprecipitation, pull-down assay, and retroviral rescue assay. We also evaluated the protective effect of VDR against *Salmonella* infection in a *Salmonella* intraperitoneal injection model.

Mice

Vdr^{flox/flox} mice were generated by (Beijing Biocytogen, China). Vdr^{-/-} C57BL/6 mice were obtained from the Jackson Laboratory. Nlrp3^{-/-} mice and Lyz2-Cre were gifts from Dr. Shuo Yang (Nanjing Medical University, China). Nlrc4^{-/-} mice were a gift from Dr. Shao Feng (NIBS). The Institutional Animal Care and Use Committee of Nanjing Medical University approved the animal experiments. The mice used were 6–8 weeks of age. All mice were bred in the Animal Core Facility of Nanjing Medical University.

Reagent

PolyJetTM DNA transfection Reagent (SL100688) was purchased from SignaGen (USA). Hieff TransTM Liposomal Transfection Reagent (40802ES02) was purchased from Yeasen Biotechnology Co., LTD (China). A Plasmid DNA Miniextraction kit (DC201-01) was purchased from Nanjing Vazyme Biotechnology Co., LTD (China). His tag Protein Purification Kit (P2226) was purchased from Beyotime (China). Anti-VDR (1:1,000, sc-13133) and Anti-β-actin (1:1,000, sc-47778) were purchased from Santa Cruz Biotechnology (Delaware, USA). TNF ELISA kit (Cat#558534), Mouse IL-1β ELISA kit (Cat#559603), TMB Substrate Reagent Set (Cat#555214) were purchased from BD Biosciences (State of New Jersey, USA). Mouse IL-18 ELISA kit (Cat# CK-E 20173) were purchased from Milbio (Shanghai, China). Anti-NLRP3/NALP3 (1:1,000, Cat# AG-20B-0014), Anti-Caspase-1 (mouse; 1:1,000, Cat# AG-20B-0044), Anti-ASC (1:1,000, Cat# sc-514414), were purchased from AdipoGen (USA). Anti-NLRC4 (human; 1:1,000) and Anti-HA (1:1,000, Cat#3724) were purchased from Cell signaling technology (Massachusetts, USA). Anti-p-NLRC4 (Ser533; 1:1,000, Cat#5411) and Anti-NLRC4 (human & mouse; 1:1,000, Cat#2994846) were purchased from ECM Biosciences (USA). Anti-GSDMD (1:1,000, ab109845) were purchased from Abcam (UK). Anti-Myc (1:1,000, Cat# MA1-980) and Anti-Flag

(1:1,000, Cat# F1804) were purchased from Sigma-Aldrich (Jefferson City, USA). Anti-IL-1β (1:1,000, Cat# AF-401-NA) were purchased from R&D Systems (Minnesota, USA).

Plasmids

CMV-HA-vector and pcNDA3.1-Flag-vector is kept by our laboratory. CMV-HA-VDR, pCMV-HA-VDR-C terminal, pCMV-HA-VDR-N terminal, pcNDA3.1-Flag-VDR, pcNDA3.1-Flag-VDR-C terminal, pcNDA3.1-Flag-VDR-N terminal, Pgex6p1-GST-VDR, pcDNA3.3-Myc-NLRC4, pcDNA3.3-Myc-CARD, pcDNA3.3-Myc-NACHT, pcDNA3.3-Myc-LRR, Pet28a-His-NLRC4 were constructed by our laboratory. Myc-PrgJ, MYC-Flagellin, HA-NAIP2, HA-NAIP5, FLAG-NLRC4, pet28-LFN-FLIC, pet28-LFN-PrgJ are gifts from Shao Feng Laboratory, Beijing Academy of Life Sciences.

Cell culture

HEK293T cell (CRL-11268) and THP1 cell (TIB-202) were purchased from ATCC. Primary bone-marrow-derived macrophages were isolated from the bone marrow of mice aged 8 weeks and cultured in DMEM supplemented with 1% penicillin/streptomycin, 10% FBS, and 10% (v/v) conditioned medium from L929 mouse fibroblasts for 5–7 days. HEKHEK293T cells were frozen in liquid nitrogen, resuscitated, and cultured in a cell incubator containing 5% CO₂ and 95% air at 37°C. For the NLRC4 inflammasome activation assay, 1 × 10⁶ cells were plated in 12-well plates overnight. Then, the cells were stimulated with PBS (mock) and *S. Typhimurium* (MOI = 10 or MOU = 50) for 2 h.

Bacterial culture

Salmonella Typhimurium strain SL1344 is a gift from Professor Liu Xingyin's lab, Nanjing Medical University. *Salmonella Typhimurium* strain SL1344 was inoculated into Luria-Bertani (LB) broth and incubated overnight under aerobic conditions at 37°C. Then subcultured it (1:50) for 3 h at 37°C in fresh LB broth to generate bacteria grown to log phase.

Protein purification

Plasmid PET28-Lfn-Flagellin, PET28-Lfn-PrgJ, and PET28 - anthrax-protective antigen (gifts from Dr. Shao Feng (NIBS)) were transformed into *Escherichia coli* strain BL21, respectively, and cultured overnight at 37°C. Single clones were selected into liquid LB medium and shaken overnight at 37°C. The bacterial solution was inoculated into mass LB at a ratio of 1:100 and cultured at 37°C. When OD600 reached 0.5–0.7, 0.5 mM IPTG was added to the bacterial solution, and the expression was induced at 22°C for 12 h.

Thallus was collected by centrifugation at 1,503g for 20 min at 4°C. After ultrasonic lysis, the purified protein was obtained according to the instructions of His tag Protein Purification Kit.

Inflammasome activation

LPS (500 ng/ml) was administered for 4 h and Nigricin (5 mM) for 45 min to stimulate NLRP3 inflammasome activation. *Salmonella* was injected intraperitoneally into mice or added directly to cells to activate the NLRP3 inflammasome. The purified protein (FLIC/PrgI) is transfected into bone marrow macrophages to activate the NLRP3 inflammasome by following the transfection reagent instructions (40802ES02).

ASC oligomerization assay

BMDM Cells were plated on 12-well plates and stimulated as indicated. Then washed, the cells three times with PBS and lysed them in PBS containing 0.5% Triton X-100 for 30 min at 4°C and centrifuged the cell lysates at 8,000 × g for 15 min at 4°C. The pellets soluble in Triton X-100 were washed twice with PBS and suspended in 200 µl of PBS, then cross-linked for 30 min by adding fresh disuccinimidyl suberate (2 mM) at room temperature. The cross-linked pellets were centrifuged at 8,000 × g for 15 min and lysed in protein loading buffer for Western blot analysis.

ELISA and LDH cytotoxicity assay

According to the manufacturer's instructions, IL-1 β, IL-18, and TNF-α concentrations in cell supernatant or mouse serum was measured by ELISA kits. LDH releases were measured by the LDH cytotoxicity detection kit (Beyotime) indicated according to the manufacturer's instructions.

Western blot

Protein lysates obtained from cell or tissue lysis were separated in a running buffer using either 10 or 12% SDS-PAGE gel and transferred to a PVDF membrane using a wet transfer system. These membranes were blocked in 5% skim milk in Tris-buffered with saline Twine (TBST) at room temperature for 1 h. After that, these membranes were incubated with primary antibodies.

Co-immunoprecipitation

The cells were lysed with RIPA cell lysate containing 1% protease inhibitor PMSF. The lysate was centrifuged at 13,523g at 4°C for 10 min. Protein content was measured by one-drop instrument, and the protein content was consistent. After the antibody was added and slowly rotated overnight at 4°C, protein A/G magnetic beads were used to precipitate the immune complex. The beads were then washed three times with 1× PBST (containing 1% Triton 100) to remove antigen nonspecific binding. The IP sample was resuspended with 1× loading buffer and boiled at 95°C for 5 min.

GST pull-down assay

The recombinant plasmid containing VDR and NLRC4 was transformed into *E. coli* BL21-CodonPlus (DE3) cells. The expression of the recombinant protein GST-VDR was induced by 0.1 mM isopropyl β-D-1-thiogalactopyranoside (IPTG) for 12 h at 20°C; 0.5 mM IPTG induced the His-NLRC4 for 14 h at 20°C. Then follow the instructions provided by GST-labeled protein purification kit or His-labeled protein purification kit (Beyotime Biotechnology) for

purification. After the purified protein was incubated in the same centrifuge tube overnight, GST/HIS antibody was added to form an immune complex with the protein. Protein A/G magnetic beads were used to precipitate the immune complex. The beads were then washed three times with 1× PBST (containing 1% Triton 100) to remove antigen nonspecific binding. The IP sample was resuspended with 1× loading buffer and boiled at 95°C for 5 min.

Retroviral rescue assay

Murine Vdr and VDRK123A were sub-cloned into the pHBLV-CMV-MCS-3XFlag-GFP-PURO lentivirus vector. A lentivirus-containing medium was obtained from Hanbio. Vdr-deficient BMDMs were plated in 12-well plates on the first day, then lentivirus containing the Vdr, VDRK123A, or empty vector was incubated with BMDMs (MOI = 50) at 37°C for 4 h. Then, the medium was replaced, and the cells were incubated for another 48 h. The cell lysates were analyzed by immunoblot.

Animal infection and survival analysis

To test Salmonella-induced survival in mice, each mouse was intraperitoneally injected with 10² CFU *S. Typhimurium*. The death time and the number of mice were observed and analyzed. To detect NLRC4 inflammatory cytokine secretion caused by acute Salmonella infection, serum samples were collected 24 h after intraperitoneal injection of 10⁴CFU *S. Typhimurium* per mouse.

Detection of Salmonella Typhimurium load

Prepare LB solid plate without any resistance in advance. The mice's spleen and other related organs were collected, weighed, and then placed in a 1.5-ml tube containing 1 ml sterile PBS buffer solution for tissue grinding (2–5 min at 60 Hz). Diluted the homogenate obtained by grinding according to gradient dilution method, and took 200 µl of mixture diluted 10³–10⁴ times. The plates were incubated a 37°C overnight. After about 14–16 h, the LB plate was taken out for taking photographs and counting. Mice were injected intraperitoneally with 10² CFU *S. Typhimurium* for survival analysis in 200 µl PBS. The death time and the number of mice were observed and analyzed.

Immunofluorescence staining

For ASC speck analysis, BMDMs were plated on coverslips. The cells were fixed with a paraformaldehyde stationary solution (Service) for 15–20 min and then permeabilized with 0.2% NP-40 for 10–15 min. Incubated them with anti-rabbit ASC antibody (1:200) overnight at 4°C, then incubated with anti-rabbit Cy3-conjugated AffiniPure (Jackson Immuno Research). Nuclei were stained by DAPI (Sigma). For co-localization analysis, HEKHEK293T cells transfected with plasmids encoding Flag-VDR and Myc-NLRC4 were cultured for 18–24 h. Then incubated with anti-Flag and anti-Myc antibodies (1:100) overnight at 4°C and incubated with fluorescent secondary antibody at room temperature for 1–2 h. The immunofluorescence staining experiment was examined by fluorescence microscopy (BX3, Olympus, Japan).

Predicted the critical binding site of VDR in the formation of the VDR–NLRC4 complex

The three-dimensional (3D) structure of the active state of NLRC4 (ΔCARD; PDB: 3JBL) is obtained from PDB (Protein Data Bank),

and the structure was optimized in MOE2019.01 through energy minimization. The homology modeling of mouse VDR C-domain was predicted by the Swiss-Model server (<https://swissmodel.expasy.org>) with the X-ray crystal structure of rat VDR (PDB code [IRKG](#), 97% identity) as the template (Vanhooke et al, 2004). The probable interaction mode of VDR–NLRC4 is explored by protein–protein docking by Molecular Operating Environment (MOE 2019.01) software with default parameters.

Statistical analyses

All data in this study were processed by GraphPad Prism 7 software. The comparison between groups was performed by *t*-test, and one-way ANOVA was performed to compare three or more groups. A *P*-value < 0.05 can be considered a statistical difference.

Data availability

This study includes no data deposited in external repositories.

Expanded View for this article is available online.

Acknowledgements

We thank Dr. Feng Shao (NIBS) for providing NLRC4^{-/-} mice and plasmids, We thanks Dr. Shou Yang (Nanjing Medical University, China) for providing NLRP3^{-/-} and Lyz2-Cre mice. This work was supported by the National Nature Science Foundation of China (NSFC) (81871310, 82171723 and 81371759), the Natural Science Foundation of Jiangsu Higher Education Institutions of China (17KJA310002), the Key Project of a Science and Technology Development Fund from Nanjing Medical University (2017NJMUCX003), the Research Start-up Fund from Nanjing Medical University (2014RC02) to YC.

Author contributions

Xin Chen: Conceptualization; data curation. **Zaikui Zhang:** Data curation. **Naishuang Sun:** Data curation. **Jin Zhou Li:** Data curation. **Zemeng Ma:** Data curation. **Zebing Rao:** Data curation. **Xiaomeng Sun:** Data curation. **Qiang Zeng:** Formal analysis. **Yuxuan Wu:** Formal analysis. **Jiahuang Li:** Formal analysis. **Jing Zhang:** Data curation; Formal analysis. **Yunzi Chen:** Conceptualization; resources; data curation; software; formal analysis; supervision; funding acquisition; validation; investigation; visualization; methodology; writing—original draft; project administration; writing—review and editing.

In addition to the [CRediT](#) author contributions listed above, the contributions in detail are:

YC, XC, ZZ, and JZ designed the research, analyzed data, and wrote the paper. ZR, NS, JL, ZM, XS QZ, and YW provided research reagents and technical assistance. JZ and JL assisted in data analysis and manuscript preparation. YC was responsible for the overall research design, data analysis, and paper preparation.

Disclosure and competing interests statement

The authors declare that they have no conflict of interest.

References

Bauer R, Rauch I (2020) The NAIP/NLRC4 inflammasome in infection and pathology. *Mol Aspects Med* 76: 100863

- Broz P, Newton K, Lamkanfi M, Mariathasan S, Dixit VM, Monack DM (2010) Redundant roles for inflammasome receptors NLRP3 and NLRC4 in host defense against Salmonella. *J Exp Med* 207: 1745–1755
- Carlberg C (2019) Vitamin D signaling in the context of innate immunity: focus on human monocytes. *Front Immunol* 10: 2211
- Duan A, Ma Z, Liu W, Shen K, Zhou H, Wang S, Kong R, Shao Y, Chen Y, Guo W et al (2021) 1,25-Dihydroxyvitamin D inhibits osteoarthritis by modulating interaction between vitamin D receptor and NLRP3 in macrophages. *J Inflamm Res* 14: 6523–6542
- Duncan JA, Canna SW (2018) The NLRC4 inflammasome. *Immunol Rev* 281: 115–123
- Gatti D, Idolazzi L, Fassio A (2016) Vitamin D: not just bone, but also immunity. *Minerva Med* 107: 452–460
- Gong YN, Shao F (2012) Sensing bacterial infections by NAIP receptors in NLRC4 inflammasome activation. *Protein Cell* 3: 98–105
- Gram AM, Wright JA, Pickering RJ, Lam NL, Booty LM, Webster SJ, Bryant CE (2021) Salmonella flagellin activates NAIP/NLRC4 and canonical NLRP3 inflammasomes in human macrophages. *J Immunol* 206: 631–640
- Ismailova A, White JH (2021) Vitamin D, infections and immunity. *Rev Endocr Metab Disord* 23: 265–277
- Kim DH, Klemp A, Salazar G, Hwang HS, Yeh M, Panton LB, Kim JS (2020) High-dose vitamin D administration and resistance exercise training attenuate the progression of obesity and improve skeletal muscle function in obese p62-deficient mice. *Nutr Res* 84: 14–24
- Lage SL, Longo C, Branco LM, da Costa TB, Buzzo Cde L, Bortoluci KR (2014) Emerging concepts about NAIP/NLRC4 inflammasomes. *Front Immunol* 5: 309
- Liu W, Chen Y, Golan MA, Annunziata ML, Du J, Dougherty U, Kong J, Musch M, Huang Y, Pekow J et al (2013) Intestinal epithelial vitamin D receptor signaling inhibits experimental colitis. *J Clin Invest* 123: 3983–3996
- Liu W, Liu X, Li Y, Zhao J, Liu Z, Hu Z, Wang Y, Yao Y, Miller AW, Su B et al (2017) LRRK2 promotes the activation of NLRC4 inflammasome during Salmonella Typhimurium infection. *J Exp Med* 214: 3051–3066
- Madanchi M, Fagagnini S, Fournier N, Biedermann L, Zeitz J, Battagay E, Zimmerli L, Vavricka SR, Rogler G, Scharl M et al (2018) The relevance of vitamin and iron deficiency in patients with inflammatory bowel diseases in patients of the Swiss IBD cohort. *Inflamm Bowel Dis* 24: 1768–1779
- Pappa H (2014) Vitamin D deficiency and supplementation in patients with IBD. *Gastroenterol Hepatol* 10: 127–129
- Qu Y, Misaghi S, Newton K, Maltzman A, Izrael-Tomasevic A, Arnott D, Dixit VM (2016) NLRP3 recruitment by NLRC4 during Salmonella infection. *J Exp Med* 213: 877–885
- Rao Z, Chen X, Wu J, Xiao M, Zhang J, Wang B, Fang L, Zhang H, Wang X, Yang S et al (2019) Vitamin D receptor inhibits NLRP3 activation by impeding its BRCC3-mediated deubiquitination. *Front Immunol* 10: 2783
- Sundaram B, Kanneganti TD (2021) Advances in understanding activation and function of the NLRC4 inflammasome. *Int J Mol Sci* 22: 1048
- Tenthorey JL, Kofoed EM, Daugherty MD, Malik HS, Vance RE (2014) Molecular basis for specific recognition of bacterial ligands by NAIP/NLRC4 inflammasomes. *Mol Cell* 54: 17–29
- Vance RE (2015) The NAIP/NLRC4 inflammasomes. *Curr Opin Immunol* 32: 84–89
- Vanhooke JL, Benning MM, Bauer CB, Pike JW, DeLuca HF (2004) Molecular structure of the rat vitamin D receptor ligand binding domain complexed with 2-carbon-substituted vitamin D3 hormone analogues and a LXLL-containing coactivator peptide. *Biochemistry* 43: 4101–4110

- Wu S, Liao AP, Xia Y, Li YC, Li JD, Sartor RB, Sun J (2010) Vitamin D receptor negatively regulates bacterial-stimulated NF-kappaB activity in intestine. *Am J Pathol* 177: 686–697
- Zhang L, Chen S, Ruan J, Wu J, Tong AB, Yin Q, Li Y, David L, Lu A, Wang WL et al (2015) Cryo-EM structure of the activated NAIP2-NLRC4 inflammasome reveals nucleated polymerization. *Science* 350: 404–409
- Zhao Y, Shao F (2015) The NAIP-NLRC4 inflammasome in innate immune detection of bacterial flagellin and type III secretion apparatus. *Immunol Rev* 265: 85–102
- Zhao Y, Yang J, Shi J, Gong YN, Lu Q, Xu H, Liu L, Shao F (2011) The NLRC4 inflammasome receptors for bacterial flagellin and type III secretion apparatus. *Nature* 477: 596–600